

# Geodesic Shape Spaces of Surfaces of Genus Zero

Xiuwen Liu, Washington Mio, Yonggang Shi, Ivo Dinov

► **To cite this version:**

Xiuwen Liu, Washington Mio, Yonggang Shi, Ivo Dinov. Geodesic Shape Spaces of Surfaces of Genus Zero. Xavier Pennec. 2nd MICCAI Workshop on Mathematical Foundations of Computational Anatomy, Oct 2008, New-York, United States. pp.105-116, 2008. <inria-00632879>

**HAL Id: inria-00632879**

**<https://hal.inria.fr/inria-00632879>**

Submitted on 16 Oct 2011

**HAL** is a multi-disciplinary open access archive for the deposit and dissemination of scientific research documents, whether they are published or not. The documents may come from teaching and research institutions in France or abroad, or from public or private research centers.

L'archive ouverte pluridisciplinaire **HAL**, est destinée au dépôt et à la diffusion de documents scientifiques de niveau recherche, publiés ou non, émanant des établissements d'enseignement et de recherche français ou étrangers, des laboratoires publics ou privés.

# Geodesic Shape Spaces of Surfaces of Genus Zero<sup>\*</sup>

Xiuwen Liu<sup>1</sup>, Washington Mio<sup>2</sup>, Yonggang Shi<sup>3</sup>, and Ivo Dinov<sup>3</sup>

<sup>1</sup> Department of Computer Science, Florida State University, Tallahassee, FL 32306

<sup>2</sup> Department of Mathematics, Florida State University, Tallahassee, FL 32306

<sup>3</sup> Laboratory of Neuro Imaging, UCLA School of Medicine, Los Angeles, CA 90095

**Abstract.** We construct shape spaces of elastic spherical surfaces immersed in Euclidean space  $\mathbb{R}^k$ . The spaces are equipped with geodesic metrics that depend on the tension and rigidity of the surfaces. We develop algorithms to calculate geodesics and geodesic distances, as well as tools to quantify local shape similarities and contrasts, thus obtaining a local-global formulation. We give examples of geodesic interpolations and illustrations of the use of the model in brain mapping.

## 1 Introduction

The development of computational models of shapes of surfaces in Euclidean space is motivated by core problems in computational anatomy such as mapping the human brain, characterizing normal variation in anatomy and identifying pathological changes. In recent years, significant progress has been made in the study of Riemannian shape spaces of curves (see e.g. [1–5]). However, a computationally feasible approach to higher-dimensional shapes still poses many challenges. In this paper, we construct a geodesic shape space of elastic surfaces of genus zero in  $\mathbb{R}^k$ , with shapes realized as piecewise linear immersions of a triangle mesh  $K$  homeomorphic to the 2-sphere. We represent a parametric shape by its discrete exterior derivative because first-order representations provide a good balance between computational tractability and geometrical accuracy. Representations beyond order zero also are more effective in capturing deformations such as elastic bends and folds. The space of immersions is equipped with a family of Riemannian metrics that reflect the elasticity properties of the surfaces. The general model is anisotropic and inhomogeneous, as it allows the tension and rigidity of a surface to vary throughout its extension. The representation is invariant under translations and a shape space of spherical surfaces is obtained by normalizing scale and accounting for the action of orthogonal transformations.

The paper is devoted to the development of the elastic shape models and algorithms to calculate geodesic paths and geodesic distances in shape space. We use these basic tools to estimate mean shapes and to construct an anatomical

---

<sup>\*</sup> This work was supported in part by NSF grants DMS-0713012 and CCF-0514743, and NIH Roadmap for Medical Research grant U54 RR021813.

atlas of the right hippocampus. Our shape model is used in conjunction with existing surface parametrization and registration techniques [6–8], but research in these areas is still ongoing and is complementary to the study of shape spaces. Although shape distance is a global measurement of shape dissimilarity, the formulation used also enables us to characterize and quantify local shape differences. This is important in applications in order to identify the regions where the most significant morphological contrasts occur. Shapes of surfaces can be studied from several other viewpoints. Alternative approaches include: (i) models based on landmark representations [9]; (ii) models that rely on diffeomorphisms acting on a volume containing a surface to describe shape deformations [10]; (iii) models based on medial-axis representations [11].

The paper is organized as follows. In Section 2, we discuss the shape representation and examine invariance under shape-preserving transformations. In Section 3, we define the elastic shape metrics. The algorithm to calculate geodesics via energy minimization is presented in Sections 4 and 5, where illustrations are also provided. Energy density functions and localization techniques are discussed in Section 6. We conclude with a summary and some discussion in Section 7.

## 2 Shape Representation

Let  $K$  be a finite simplicial complex whose underlying polyhedron  $|K|$  is homeomorphic to the unit 2-sphere  $\mathbb{S}^2$ .  $K$  will be fixed throughout the discussion. A parametric spherical shape will be realized as a mapping  $\alpha: |K| \rightarrow \mathbb{R}^k$ , which is linear on each simplex of  $K$ . Thus, if  $V = \{z_1, \dots, z_p\}$  is the vertex set of  $K$ ,  $\alpha$  is completely determined by its restriction  $\alpha: V \rightarrow \mathbb{R}^k$  to  $V$ . Next, we define the discrete exterior derivative  $d\alpha$ , which is a measure of the variation of  $\alpha$  along the edges of  $K$ . Fix an orientation for each edge and each triangle of  $K$  and let  $E = \{e_1, \dots, e_m\}$  and  $F = \{T_1, \dots, T_n\}$  be the oriented edge and face sets of  $K$ . For an oriented edge  $e$ , let  $e^-$  and  $e^+$  denote its initial and terminal vertices, respectively. Then,  $d\alpha: E \rightarrow \mathbb{R}^k$  is given by  $d\alpha(e_i) = \alpha(e_i^+) - \alpha(e_i^-)$ . Note that it suffices to define  $d\alpha$  over the oriented edges in  $E$  because if we reverse the orientation of an edge, the variation of  $\alpha$  gets multiplied by  $-1$ . We only consider mappings such that  $d\alpha(e_i) \neq 0$ , for every  $e_i \in E$ , which we refer to as *immersions*. This just means that no edge gets crushed to a point under  $\alpha$ . For each  $i$ ,  $1 \leq i \leq m$ , we write the modular component of  $d\alpha(e_i)$  in logarithmic scale as  $r_i = \log \|d\alpha(e_i)\|$  and the directional component as  $v_i = d\alpha(e_i) / \|d\alpha(e_i)\|$ . Thus, the (oriented)  $i$ th edge of  $\alpha$  is represented by the vector  $e^{r_i} v_i$ . Writing each  $v_i$  as a row vector  $v_i = [v_{i1} \dots v_{ik}]$ , the parametric surface  $\alpha$  will be represented by the pair  $(r, v) \in \mathbb{R}^m \times \mathbb{R}^{m \times k}$ , where  $r = [r_1 \dots r_m]^T$  and  $v$  is the  $m \times k$  matrix whose  $i$ th row is  $v_i$ . Since the Riemannian metrics on  $\mathbb{R}^m \times \mathbb{R}^{m \times k}$  to be used in the development of our shape models differ from the standard Euclidean metric, we will use the notation  $\mathbb{E}$  for this space to emphasize this fact. Thus,  $\mathbb{E}$  is the space of dimension  $m(k+1)$  formed by all pairs  $(r, v)$ , with the topology induced by the Euclidean metric. Thus far, the only constraint on  $(r, v)$  is that

each row of  $v$  must be a unit vector. We denote by  $M$  the subspace of  $\mathbb{E}$  formed by all pairs  $(r, v)$  with this property.

### 2.1 Pre-Shape Space

The representation of  $\alpha$  via  $(r, v)$  is clearly invariant under translations. To fix scale, we set the total edge length to be unitary; that is, we normalize the pair  $(r, v)$  to satisfy

$$G_1(r, v) = \sum_{i=1}^m e^{r_i} = 1. \tag{1}$$

*Remark.* Alternatively, one may normalize scale by fixing the total area, or simply drop this condition if a scale-sensitive model is desired.

What pairs  $(r, v)$  represent the exterior derivative of a mapping  $\alpha: |K| \rightarrow \mathbb{R}^k$ ? The integrability conditions will reveal the further constraints to be imposed on  $(r, v)$ . If  $p$  is an oriented path in  $K$  formed by a sequence of oriented edges, let the integer  $n_i$  be the net number of times that the oriented edge  $e_i \in E$  is traversed by  $p$ , where a negative sign indicates reversal of orientation. Given an immersion  $\alpha$ , its variation along  $p$  may be expressed as  $\sum_{i=1}^m n_i d\alpha(e_i) = \sum_{i=1}^m n_i e^{r_i} v_i$ . The variation of  $\alpha$  along any (oriented) cycle  $c$  in  $K$  clearly must vanish. Conversely, given  $(r, v)$ , define the integral of  $(r, v)$  along the path  $p$  to be  $I(p) = \sum_i n_i e^{r_i} v_i$ . If  $I(c)$  vanishes along every cycle  $c$ , then  $(r, v)$  represents the exterior derivative of some  $\alpha$ , uniquely determined up to translations. This can be seen as follows: fix a vertex  $v_0$  of  $K$  and a point  $x_0 \in \mathbb{R}^k$  and define  $\alpha(v_0) = x_0$ . For any other vertex  $v$ , choose a path  $p$  from  $v_0$  to  $v$  and let  $\alpha(v) = x_0 + I(p)$ . The vanishing condition over cycles ensures that  $\alpha(v)$  is independent of the path chosen.

Verifying that  $I(c) = 0$ , for every cycle  $c$ , is not computationally feasible. However, it suffices to check this vanishing condition on cycles that are boundaries of oriented triangles (this uses the fact that the 2-sphere is simply connected). This is because the integral along any cycle in  $K$  can be accounted for by combining the integrals along the boundaries of appropriately chosen oriented triangles. For each oriented triangle  $T_\ell \in F$ , let  $\varepsilon_{\ell_1} e_{\ell_1}, \varepsilon_{\ell_2} e_{\ell_2}, \varepsilon_{\ell_3} e_{\ell_3}$  be the oriented edges of  $T_\ell$ , where  $\varepsilon_{\ell_i} = \pm 1, e_{\ell_i} \in E$ , and the indexes satisfy  $\ell_1 < \ell_2 < \ell_3$ . Then, the argument above shows that a pair  $(r, v)$  represents the exterior derivative of an immersion  $\alpha$  if and only if it satisfies the following  $kn$  integrability conditions:

$$G_{\ell,j}(r, v) = \sum_{i=1}^3 \varepsilon_{\ell_i} e^{r_{\ell_i}} v_{\ell_i,j} = 0. \tag{2}$$

where  $1 \leq \ell \leq n$  and  $1 \leq j \leq k$ . It is not difficult to see that one may drop condition (2) over one of the triangles, say  $T_n$ , since the variation along the boundary of any of the triangles can be expressed as a combination of the variations along the boundaries of the remaining ones. Thus, we obtain  $k(n - 1)$  independent integrability conditions.

Pairs  $(r, v) \in M$  satisfying (1) and (2) will be called *pre-shapes* and the space of all pre-shapes will be denoted  $P$ . A pre-shape gives a representation of immersions that is invariant to scale and translations. Thus, we have introduced

a nested sequence  $P \subset M \subset \mathbb{E}$  of spaces, which will be useful at various stages of our constructions.

*Remark.* A more formal explanation of the integrability of  $(r, v)$  can be given in terms of simplicial cohomology. The vanishing of the integral of  $(r, v)$  along the boundaries of oriented triangles means that the simplicial 1-cochain (with coefficients in  $\mathbb{R}^k$ ) determined by  $e_i \mapsto e^{r_i} v_i$ ,  $1 \leq i \leq m$ , is a 1-cocycle. This cocycle represents the trivial cohomology class because  $|K|$  is simply connected. Thus, the cocycle is integrable. This interpretation also allows us to identify the further integrability conditions needed for a complex  $K$  of different topology. The details will be discussed in future work.

## 2.2 Shape Space

Let  $O(k)$  be the group of  $k \times k$  orthogonal matrices. If  $U \in O(k)$  and  $\alpha$  is an immersion, the result of applying the rigid transformation  $U$  to  $\alpha$  is the composition  $U \circ \alpha: V \rightarrow \mathbb{R}^k$ . The induced action on  $(r, v)$  is  $(r, v) \mapsto (r, vU^T)$ . The action on the modular component is trivial because edge lengths do not change under  $U$ . Pre-shapes clearly get transformed into pre-shapes and the orbit of  $(r, v)$  is  $\mathcal{O}(r, v) = \{(r, vU^T) : U \in O(k)\}$ . Since pre-shapes that differ by a rigid transformation have the same shape, we define the shape space  $S$  as the orbit space of  $P$  under the action of  $O(k)$ . In other words, as the quotient  $S = P/O(k)$ .

## 3 Riemannian Metrics

We introduce Riemannian structures on  $\mathbb{E}$  that will lead to a family of elastic pre-shape and shape metrics. The general model is anisotropic and inhomogeneous, but the family contains a special 1-parameter homogeneous class. The idea is that each edge of a shape may offer different resistance to stretching/compression and bending, which will be quantified by its tension and rigidity coefficients. The geodesic distance will be related to the minimum energy required to deform a shape into another under these conditions.

Let  $a, b: E \rightarrow \mathbb{R}^+$  be positive functions defined on the edge set, where  $a_i = a(e_i)$  and  $b_i = b(e_i)$  represent the tension and rigidity coefficients of the  $i$ th edge. Consider the Riemannian structure on  $\mathbb{E}$  given at  $(r, v)$  by

$$\langle (h, w), (\bar{h}, \bar{w}) \rangle_{(r, v)} = \sum_{i=1}^m a_i h_i \bar{h}_i e^{r_i} + \sum_{i=1}^m b_i (w_i \cdot \bar{w}_i) e^{r_i}. \quad (3)$$

If we think of  $(h, w)$  as an infinitesimal deformation of  $(r, v)$ , then  $\|(h, w)\|_{(r, v)}^2 = \langle (h, w), (h, w) \rangle_{(r, v)}$  is the energy cost of the deformation. Henceforth, the sub-manifolds  $P$  and  $M$  will have the Riemannian structure induced from (3). If  $(r, v)$  and  $(\bar{r}, \bar{v})$  are pre-shapes, we let  $\delta((r, v), (\bar{r}, \bar{v}))$  be the geodesic distance

between them on the pre-shape manifold  $P$ . If  $s$  and  $\bar{s}$  are the shapes associated with the orbits of  $(r, v)$  and  $(\bar{r}, \bar{v})$ , the shape distance is defined as

$$d(s, \bar{s}) = \inf_{U, V \in O(k)} \delta((r, vV^T), (\bar{r}, \bar{v}U^T)) = \inf_{U \in O(k)} \delta((r, v), (\bar{r}, \bar{v}U^T)). \quad (4)$$

The last equality follows from the fact that the Riemannian metric is compatible with the action of  $O(k)$ ; that is,  $O(k)$  acts by isometries. Most of the remaining work will be devoted to the calculation of geodesics in  $P$  and the geodesic distance  $\delta$ . The minimization over  $O(k)$  is a relatively simpler calculation, as indicated below.

## 4 Path Spaces and the Energy Functional

Our next goal is to construct a pre-shape geodesic between  $(r, v), (\bar{r}, \bar{v}) \in P$ . The idea is to begin with a path in  $P$  connecting the pre-shapes and gradually deform it to a geodesic following the negative gradient flow of the path energy. Implicit in this statement is that a path space equipped with a Riemannian structure has been constructed.

### 4.1 Path Spaces

Let  $I = [0, 1]$ . If  $p: I \rightarrow M$  is a path in  $M$ , we write its modular and directional components as  $p(t) = (r^t, v^t)$ . Let  $Y$  be the manifold of all absolutely continuous paths in  $M$  (with square integrable derivative). A tangent vector to  $Y$  at  $p$  represents an infinitesimal deformation of the path and is given by a vector field  $(h^t, w^t)$  along  $p$  with the property that  $w_i^t \cdot v_i^t = 0$ , for every  $1 \leq i \leq m$  and  $\forall t \in I$ . This follows from the fact that  $\|v_i^t\|^2 = 1$  so that the deformation of each  $v_i^t$  has to be tangential to the unit sphere. Consider the Riemannian metric on the path space  $Y$  given by

$$\langle (h, w), (\bar{h}, \bar{w}) \rangle_p = \langle (h^0, w^0), (\bar{h}^0, \bar{w}^0) \rangle_{p(0)} + \int_0^1 \langle D_t (h^t, w^t), D_t (\bar{h}^t, \bar{w}^t) \rangle_{p(t)} dt, \quad (5)$$

where  $D_t$  denotes covariant differentiation in  $M$  along  $p$ . This type of inner product in function space was, to our knowledge, introduced by Palais [12]. Motivated by the inclusion  $P \subset M$ , we consider the following submanifolds of  $Y$ :

- (i) The space  $Z_M \subset Y$  of paths in  $M$  satisfying the boundary conditions  $p(0) = (r, v)$  and  $p(1) = (\bar{r}, \bar{v})$ .
- (ii) The space  $Z_P \subset Z_M$  of paths in the pre-shape space  $P$  satisfying the boundary conditions described in (i). A path in  $Z_P$  has the property that each  $(r^t, v^t)$  also satisfies (1) and (2).

We thus have three nested path spaces:  $Z_P \subset Z_M \subset Y$ .

## 4.2 The Energy Functional

On the path space  $Y$ , define the energy functional  $E: Y \rightarrow \mathbb{R}$  by

$$E(p) = \frac{1}{2} \int_0^1 \langle (\partial_t r^t, \partial_t v^t), (\partial_t r^t, \partial_t v^t) \rangle_{p(t)} dt. \quad (6)$$

A pre-shape geodesic between  $(r, v), (\bar{r}, \bar{v}) \in P$  is a path  $p \in Z_P$ , which is a critical point of the energy  $E$  restricted to  $Z_P$ . We are particularly interested in minimal energy paths since they represent minimal-length geodesics. We exploit the inclusions  $Z_P \subset Z_M \subset Y$  in our approach to the minimization problem, the point being that it is easier to calculate the gradient of  $E$  as a functional on  $Z_M$ . The use of (5) leads to a particularly elegant and computationally robust expression for the gradient.

## 5 Geodesics

In this section, we develop an algorithm to calculate a geodesic in  $P$  between two pre-shapes  $(r, v)$  and  $(\bar{r}, \bar{v})$  using a gradient search to minimize the energy.

### 5.1 Initialization

To initialize the process, let  $\alpha, \bar{\alpha}: V \rightarrow \mathbb{R}^k$  be immersions of  $K$  associated with  $(r, v)$  and  $(\bar{r}, \bar{v})$ , respectively. We linearly interpolate  $\alpha$  and  $\bar{\alpha}$  to obtain a 1-parameter family of mappings  $\alpha_t: K \rightarrow \mathbb{R}^k$ . If  $d\alpha_t(e_i) = 0$ , we gently deform  $\alpha_t$  to make it non-singular and then scale each  $\alpha_t$  to turn  $d\alpha_t$  into a pre-shape. The path  $p(t) = d\alpha_t$  is used to initialize the search.

### 5.2 Covariant Integration and Parallel Transport

To calculate the gradient of  $E$  at  $p$ , we first discuss covariant integration in  $M$  of a vector field  $(f^t, x^t)$  along a path  $p(t) = (r^t, v^t)$ , where  $f^t$ , where  $x^t$  denote the modular and directional components of the field. The tangentiality to  $M$  of the field  $(f^t, x^t)$  just means that  $x_i^t \cdot v_i^t = 0, \forall t \in I$  and every  $i, 1 \leq i \leq m$ . As shown in Appendix B, a vector field  $(F^t, X^t)$  along  $p$  is tangential to  $M$  and is a *covariant integral* of  $(f^t, x^t)$  if and only if it satisfies the system of differential equations

$$\begin{cases} \partial_t F_i^t = f_i^t - \frac{1}{2}(\partial_t r_i^t)F_i^t + \frac{1}{2} \frac{b_i}{a_i}(X_i^t \cdot \partial_t v_i^t) \\ \partial_t X_i^t = x_i^t - \frac{1}{2}(X_i^t \partial_t r_i^t + F_i^t \partial_t v_i^t) - (X_i^t \cdot \partial_t v_i^t)v_i^t. \end{cases} \quad (7)$$

Numerical integration of (7) with initial conditions  $(F^0, X^0)$  will be used in the calculation of geodesics. In the special case where the field  $(f^t, x^t)$  is identically zero, the integral field  $(F^t, X^t)$  is the *parallel transport* of  $(F^0, X^0)$  along  $p$ .

### 5.3 The Gradient of the Energy

Given a path  $p \in Z_P$ , we first calculate the gradient of  $E$  at  $p$  as a functional on the path space  $Y$ . For this purpose, we consider a variation  $(r^t(\mu), v^t(\mu))$  of  $p(t) = (r^t, v^t)$  in  $Y$  along a direction  $(h^t, w^t)$ , where  $\mu \in (-\epsilon, \epsilon)$  is the variation parameter. This means that  $(r^t(0), v^t(0)) = (r^t, v^t)$ , the path  $(r^t(\mu), v^t(\mu)) \in Y$  for each fixed  $\mu$ ,

$$h^t = \frac{\partial}{\partial \mu} r^t(\mu)|_{\mu=0} \quad \text{and} \quad w^t = \frac{\partial}{\partial \mu} v^t(\mu)|_{\mu=0}. \quad (8)$$

Differentiating (6) at  $\mu = 0$ , we obtain

$$dE_p(h^t, w^t) = \int_0^1 \langle D_t(h_t, w_t), (\partial_t r^t, \partial_t v^t) \rangle_{p(t)} dt,$$

where  $D_t$  denotes covariant derivative. If we set  $(f^t, x^t) = (\partial_t r^t, \partial_t v^t)$  in (7) and integrate the system with initial condition  $(F^0, X^0) = (0, 0)$ , we get a vector field  $(F^t, X^t)$  along the path  $p$ . Then, we may rewrite the variation  $dE_p(h^t, w^t)$  as

$$dE_p(h^t, w^t) = \langle (h^t, w^t), (F^t, X^t) \rangle_p. \quad (9)$$

Thus, the gradient of  $E$  at  $p$  as a functional on  $Y$  is  $\nabla_Y E(p) = (F^t, X^t)$ . To obtain  $\nabla_{Z_M} E(p)$ , we project  $\nabla_Y E(p)$  orthogonally onto the tangent space of  $Z_M$  at  $p$  with respect to the inner product (5). Since the space  $Z_M$  is obtained from  $Y$  by imposing the boundary conditions  $(r^0, v^0) = (r, v)$  and  $(r^1, v^1) = (\bar{r}, \bar{v})$  on paths, a tangent vector to  $Y$  at  $p$  is tangent to  $Z_M$  if and only if it vanishes at  $t = 0$  and  $t = 1$ . A simple (covariant) integration by parts argument shows that the orthogonal complement of the tangent space of  $Z_M$  in the tangent space of  $Y$  at  $p$  is formed by the covariantly linear fields (that is, smooth fields with trivial second covariant derivative) in  $M$  along  $p$ . By construction, the field  $(F^t, X^t)$  vanishes at  $t = 0$ . Thus, to orthogonally project  $(F^t, X^t)$  onto the tangent space of  $Z_M$ , we simply need to subtract from  $(F^t, X^t)$  the covariantly linear field that vanishes at  $t = 0$  and coincides with  $(F^t, X^t)$  at  $t = 1$ . Again, we resort to covariant integration, this time applied to the reverse of the path  $p$ . First, construct a covariant field by integrating the everywhere zero field with initial condition  $(F^1, X^1)$  along the reverse of the path  $p$ . Reversing the path again, after integration, we obtain a parallel field  $(G^t, Y^t)$  along  $p$  whose value at  $t = 1$  is  $(F^1, X^1)$ . The field  $(tG_t, tY_t)$  is covariantly linear with the desired properties. Therefore, the gradient is given by

$$\nabla_{Z_M} E(p) = \nabla_Y E(p) - (tG_t, tY_t). \quad (10)$$

Our goal is to minimize  $E$  on the path space  $Z_P$ . One possible approach is to calculate  $\nabla_{Z_P} E(p)$ , which would allow us to implement a gradient descent directly in  $Z_P$ . However, in this case, the calculation is quadratic in the number  $m = |E|$  of edges. This is undesirable as spherical meshes used in neuroimaging often have a large number of edges. Thus, we employ an alternative numerical strategy that scales linearly with  $m$  and is based on the replacement of gradient descent in  $Z_P$  by its counterpart in  $Z_M$  followed by a closest-shape projection onto  $Z_P$ . The projection algorithm is discussed in Appendix A.



### 5.4 Pre-shape Geodesics

We now present an algorithm to estimate a pre-shape geodesic from  $(r, v)$  to  $(\bar{r}, \bar{v})$ . Let  $\epsilon, \delta > 0$  be small real numbers:

- (i) Initialize the search with a path  $p(t) = (r^t, v^t)$  in  $Z_P$ , e.g., as described in Section 5.
- (ii) Let  $(f^t, x^t) = (\partial_t r^t, \partial_t v^t)$ . Using (7), integrate this field covariantly along the path  $p$  with zero initial condition. The integral field  $(F^t, X^t)$  gives the gradient  $\nabla_Y E(p)$ .
- (iii) Using (7), calculate the parallel transport of  $(F^1, X^1)$  along the reverse of the path  $p$ . Reverse the path and the parallel field again to obtain a parallel field  $(G^t, Y^t)$  along  $p$ . By (10), the  $Z_M$ -gradient of  $E$  is  $\nabla_{Z_M} E(p) = \nabla_Y E(p) - (tG_t, tY_t)$ .
- (iv) Write the modular and the directional components of the gradient  $\nabla_{Z_M} E(p)$  as  $(h^t, w^t)$ ,  $0 \leq t \leq 1$ . Update  $p(t) = (r^t, v^t)$  as a path in  $Z_M$  according to (a)  $\tilde{r}^t = r^t - \epsilon h^t$ ; (b)  $\tilde{v}_i^t = v_i^t$ , if  $w_i^t = 0$ ; (c)  $\tilde{v}_i^t = \cos(\epsilon \|w_i^t\|) v_i^t - \frac{\sin(\epsilon \|w_i^t\|)}{\|w_i^t\|} w_i^t$ , otherwise. Note that the update of  $v_i^t$  takes place along great circles of the unit sphere in  $\mathbb{R}^k$  ensuring that each  $\tilde{v}_i^t$  is a unit vector.
- (v) Project each  $(\tilde{r}^t, \tilde{v}^t)$  onto the pre-shape space  $P$  (see Appendix A) to obtain a path  $(r^t, v^t)_{\text{new}}$  in  $P$ .
- (vi) Iterate the process until  $\|(r^t, v^t)_{\text{new}} - (r^t, v^t)\|_p < \delta$ , where  $\|\cdot\|_p$  denotes the Palais norm defined in (5).

### 5.5 Shape Geodesic and Shape Distance

The geodesic shape metric defined in (4) involves a minimization of the pre-shape distance over the orthogonal group  $O(k)$ . We briefly indicate how the minimization problem can be treated. We obtain an initial estimate of

$$\hat{U} = \operatorname{argmin}_{U \in O(k)} \delta((r, v), (\bar{r}, \bar{v}U^T)), \quad (11)$$

for example, by minimizing  $\|(r, v) - (\bar{r}, \bar{v}U^T)\|_{(r,v)}^2$ . This is the same as minimizing  $\sum_{i=1}^m b_i \|v_i - \bar{v}_i U^T\|^2 e^{r_i}$ , which is equivalent to maximizing the expression  $\sum_{i=1}^m (b_i e^{r_i/2} v_i) \cdot (\bar{v}_i U^T)$ . This problem is analogous to the one that arises in Procrustes alignment of shapes [9] and admits a closed form solution. Once this initial estimate is obtained, a gradient search can be used to locally refine the estimation. Using the algorithm to calculate pre-shape distances, we compute the  $O(k)$ -gradient numerically via finite differences using the Lie group structure of  $O(k)$ .

Figures 1(a) and (b) show geodesics between cortical surfaces with 122,880 edges and hippocampal surfaces with 30,720 edges. The geodesic interpolations were calculated with homogeneous elasticity coefficients  $a_i = 0.3$ ,  $b_i = 0.7$  for the cortices and  $a_i = 0.15$ ,  $b_i = 0.85$  for the hippocampal surfaces. Correspondences between the shapes were established with the direct mapping techniques of [7, 8] and the shapes were parameterized with the methods of [6]. Figure 2 further illustrates the method with the calculation of the sample Fréchet mean shape of 8 hippocampal surfaces.

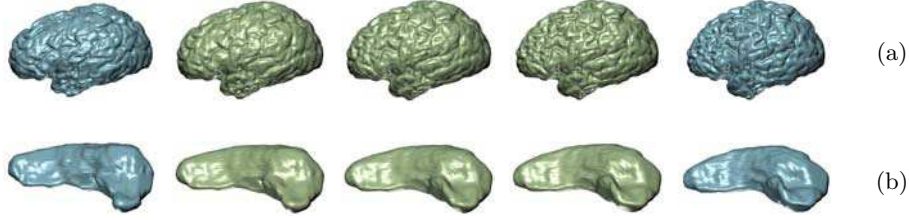


**Fig. 1.** (a) Two cortical surfaces extracted from MR images and three intermediate stages of a geodesic interpolation with homogeneous coefficients  $a_i = 0.3$  and  $b_i = 0.7$ ; (b) a similar calculation with hippocampal surfaces with  $a_i = 0.15$  and  $b_i = 0.85$ .



**Fig. 2.** The mean of 8 right hippocampal surfaces calculated with homogeneous coefficients  $a_i = 0.15$  and  $b_i = 0.85$ . The mean shape is shown on the last panel.

## 6 Energy and Localization

A pre-shape geodesic  $p(t) = (r^t, v^t)$ ,  $0 \leq t \leq 1$ , has parallel velocity field. In particular, it is traversed with constant speed  $\omega$ , where  $\omega$  is the length of  $p$ . Thus, the energy of  $p$  is  $E(p) = \int_0^1 \|\partial_t p(t)\|_{p(t)}^2 dt = \omega^2$ . On the other hand, we can write the energy as

$$E(p) = \sum_{i=1}^m \int_0^1 (a_i |\partial_t r_i^t|^2 e^{r_i} + b_i \|\partial_t v_i^t\|^2 e^{r_i}) dt, \quad (12)$$

which expresses  $E(p)$  as a sum of the local contributions of the edges. Thus, the energy density function

$$\rho(e_i) = \frac{1}{\omega^2} \int_0^1 (a_i |\partial_t r_i^t|^2 e^{r_i} + b_i \|\partial_t v_i^t\|^2 e^{r_i}) dt \quad (13)$$

quantifies the fraction of the total deformation energy associated with the  $i$ th edge. Although geodesic distance is a global quantifier of shape difference, the energy density provides a means to measure local shape differences and identify the regions where shape similarity and divergence are most pronounced. One can further decompose the local energy into its tension and rigidity components to separately quantify the local shape differences due to stretching and bending. One may also modify  $\rho$  to a function defined on the vertex set by letting the value on a vertex be the average value of  $\rho$  on the edges incident with that vertex. Figures 3 displays the initial shapes of the geodesics in Figure 1 overlaid with color maps of the respective energy density functions.



**Fig. 3.** Plots of the energy density functions for the geodesics shown in Figure 1.

## 7 Summary and Discussion

We constructed a shape space of elastic spherical surfaces immersed in Euclidean space equipped with a family of geodesic metrics that depend on the elasticity of the surfaces. The metrics reflect the resistance offered by the shapes to deformations by stretching and bending. Although the general model is anisotropic, a special homogeneous sub-collection associated with constant tension and rigidity coefficients should be of particular interest in applications. The selection of elasticity parameters for a particular problem based on shape discrimination or other criteria requires further study. We developed an algorithm to calculate geodesics between spherical shapes and introduced energy density functions that provide a localization tool that allows us to identify the regions where shape dissimilarity is most pronounced. Energy density functions also let us characterize the nature of the local elastic deformations as due to stretching or bending.

We illustrated the applicability of the methods with the calculation of geodesic deformations between pairs of cortical and hippocampal surfaces segmented from MR images. Geodesic distances, geodesic interpolations, and models of shape variation developed in shape space enable us to quantify and visualize anatomical resemblance and divergence between individuals and across populations. We applied the methods developed in the paper to the construction of an atlas of the right hippocampus as the sample Fréchet mean shape of a group of 8 segmented hippocampi. Further statistical modeling of the shape of surfaces, extensions of the model to non-spherical shapes, and applications of the computational models to problems in neuroimaging are some of the topics to be investigated in future work.

## References

1. Younes, L.: Computable elastic distance between shapes. *SIAM Journal of Applied Mathematics* **58** (1998) 565–586
2. Michor, P., Mumford, D.: Riemannian geometries on spaces of plane curves. *J. Eur. Math. Soc.* **8** (2006) 1–48
3. Klassen, E., Srivastava, A., Mio, W., Joshi, S.: Analysis of planar shapes using geodesic paths on shape manifolds. *IEEE Trans. on Pattern Analysis and Machine Intelligence* **26** (2004) 372–383
4. Mio, W., Srivastava, A., Joshi, S.: On shape of plane elastic curves. *Int. Journal of Computer Vision* **73**(3) (2007) 307–324
5. Michor, P., Mumford, D., Shah, J., Younes, L.: A metric on shape space with explicit geodesics. *arXiv:0706.4299v1* (2007)

6. Praun, E., Hoppe, H.: Spherical parametrization and remeshing. In: ACM SIG-GRAPH 2003. (2003) 340–349
7. Shi, Y., Thompson, P., Dinov, I., Osher, S., Toga, A.: Direct cortical mapping via solving partial differential equations on implicit surfaces. *Medical Image Analysis* **11**(3) (2007) 207–223
8. Shi, Y., Thompson, P., Zubicaray, G., Ross, S., Tu, Z., Dinov, I., Toga, A.: Direct mapping of hippocampal surfaces with intrinsic shape context. *NeuroImage* **36**(3) (2007) 792–807
9. Kendall, D.G.: Shape manifolds, Procrustean metrics and complex projective spaces. *Bulletin of London Mathematical Society* **16** (1984) 81–121
10. Grenander, U., Miller, M.I.: Computational anatomy: An emerging discipline. *Quarterly of Applied Mathematics* **LVI**(4) (1998) 617–694
11. Fletcher, P., Lu, C., Pizer, S., Joshi, S.: Principal geodesic analysis for the study of nonlinear statistics of shape. *IEEE Transactions on Medical Imaging* **23**(8) (2004) 995–1005
12. Palais, R.S.: Morse theory on Hilbert manifolds. *Topology* **2** (1963) 299–340
13. do Carmo, M.P.: *Riemannian Geometry*. Birkhauser (1994)

## A Closest-Shape Projection

Given  $(r, v) \in M$  near the pre-shape space  $P$ , we need an efficient estimation of the pre-shape closest to  $(r, v)$ . Consider the  $kn + 1$  residual functions  $\rho_1(r, v) = 1 - G_1(r, v)$  and  $\rho_{\ell,j}(r, v) = -G_{\ell,j}(r, v)$ , whose vanishing is equivalent to  $(r, v) \in P$ . We estimate the closest pre-shape using Newton’s method to find the zeros of  $H(r, v) = \frac{1}{2}\rho_1^2(r, v) + \frac{1}{2}\sum_{\ell,j}\rho_{\ell,j}^2(r, v)$ . If we relax the condition that each row of  $v$  must satisfy  $\|v_i\| = 1$  and just treat each  $v_i$  as an arbitrary vector in  $\mathbb{R}^k$ , then the negative gradient of  $H$  is

$$-\nabla H(r, v) = \rho_1(r, v)\nabla G_1(r, v) + \sum_{\ell,j}\rho_{\ell,j}(r, v)\nabla G_{\ell,j}(r, v), \quad (14)$$

where  $\nabla G_1^r(r, v) = [1/a_1 \dots 1/a_m]^T$  is the modular component of  $\nabla G_1(r, v)$  and the directional component is zero. The modular part of  $\nabla G_{\ell,j}(r, v)$  and the  $j$ th column of its directional component, which is its only nonzero column, are

$$\left[0 \quad \frac{\varepsilon_{\ell_1}}{a_{\ell_1}}v_{\ell_1,j} \quad 0 \quad \frac{\varepsilon_{\ell_2}}{a_{\ell_2}}v_{\ell_2,j} \quad 0 \quad \frac{\varepsilon_{\ell_3}}{a_{\ell_3}}v_{\ell_3,j} \quad 0\right]^T \quad \text{and} \quad \left[0 \quad \frac{\varepsilon_{\ell_1}}{b_{\ell_1}} \quad 0 \quad \frac{\varepsilon_{\ell_2}}{b_{\ell_2}} \quad 0 \quad \frac{\varepsilon_{\ell_3}}{b_{\ell_3}} \quad 0\right]^T. \quad (15)$$

Here, the nonzero entries occur in rows  $\ell_1$ ,  $\ell_2$  and  $\ell_3$ . Write the modular and directional parts of the gradient as  $-\nabla H(r, v) = (\delta^r, \bar{\delta}^v)$ . To make  $\bar{\delta}_i^v$  tangential to  $\mathbb{S}^2$  at  $v^i$ , replace it with  $\delta_i^v = \bar{\delta}_i^v - (\bar{\delta}_i^v \cdot v_i)v_i$ . Letting  $\epsilon(r, v) = H(r, v)/\|(\delta_1, \delta_2)\|_{(r,v)}^2$ , update  $(r, v)$  as follows:

$$\begin{cases} r = r + \epsilon\delta_1; \\ v_i = \cos(\epsilon\|\delta_i^v\|)v_i + \frac{\sin(\epsilon\|\delta_i^v\|)}{\|\delta_i^v\|}\delta_i^v, \quad \text{if } \delta_i^v \neq 0; \end{cases} \quad (16)$$

and  $v_i$  stays unchanged, otherwise. Iterate until  $H(r, v)$  becomes small.

## B Covariant Integration

For  $(z, y) = (z, y_1, \dots, y_k) \in \mathbb{R} \times \mathbb{R}^k$ , we use the subscript 0 to identify the  $z$ -coordinate and the subscript  $j$ ,  $1 \leq j \leq k$ , for the coordinate  $y_j$ . Given  $a_i, b_i > 0$ , define a Riemannian metric on  $\mathbb{R} \times \mathbb{R}^k$  whose metric tensor at  $(z, y)$  is  $g_{00}(z, y) = a_i e^z$ ,  $g_{jj}(z, y) = b_i e^z$ , and 0, otherwise. Then, the Riemannian structure on  $\mathbb{E}$ , defined in Section 3, is isometric to the Cartesian product of these  $(k+1)$ -dimensional models over  $1 \leq i \leq m$ . Thus, to derive the differential equation that governs covariant integration along a path in  $M$ , it suffices to derive the corresponding differential equation for covariant integration in  $\mathbb{R} \times \mathbb{S}^{k-1}$  with respect to the induced metric. The Christoffel symbols of the Levi-Civita connection on  $\mathbb{R} \times \mathbb{R}^k$  are  $\Gamma_{00}^0 = \Gamma_{0j}^j = \Gamma_{j0}^j = 1/2$ ,  $\Gamma_{jj}^0 = -b_i/2a_i$ ,  $1 \leq j \leq k$ , and zero otherwise. Therefore (cf. [13]), the covariant derivative of a vector field  $(F^t, X^t)$  along a path  $(z^t, y^t)$  in  $\mathbb{R} \times \mathbb{R}^k$  is given by

$$\begin{cases} D_t F^t = \partial_t F^t + \frac{1}{2}(\partial_t z^t)F^t - \frac{1}{2} \frac{b_i}{a_i} [X^t \cdot \partial_t y^t] \\ D_t X^t = \partial_t X^t + \frac{1}{2}(X^t \partial_t z^t + F^t \partial_t y^t) . \end{cases} \quad (17)$$

If  $(z^t, y^t)$  is a path in  $\mathbb{R} \times \mathbb{S}^{k-1}$ , then fields that are tangential to  $\mathbb{R} \times \mathbb{S}^{k-1}$  are those that satisfy the additional orthogonality condition  $F^t \cdot y^t = 0$ . Thus, if  $(f^t, x^t)$  and  $(F^t, X^t)$  are both tangential to  $\mathbb{R} \times \mathbb{S}^{k-1}$ , the fact that the covariant derivative of  $(F^t, X^t)$  in the submanifold  $\mathbb{R} \times \mathbb{S}^{k-1}$  is  $(f^t, x^t)$  may be rephrased as  $D_t F^t = f^t$  and  $D_t X^t = x^t + \tau^t y^t$ , where  $\tau^t$  is a scalar field to be determined. Substituting in (17), we obtain

$$\begin{cases} \partial_t F^t = f^t - \frac{1}{2} \partial_t z^t F^t + \frac{1}{2} \frac{b_i}{a_i} [X^t \cdot \partial_t y^t] \\ \partial_t X^t = x^t - \frac{1}{2}(X^t \partial_t z^t + F^t \partial_t y^t) + \tau^t y^t . \end{cases} \quad (18)$$

Differentiating  $X^t \cdot y^t = 0$ , we get  $\partial_t X^t \cdot y^t = -X^t \cdot \partial_t y^t$ . From (18), it follows that  $\tau^t = -X^t \cdot \partial_t y^t$ , where we used the facts that  $X^t \cdot y^t = 0$  and  $\partial_t y^t \cdot y^t = 0$ . Substituting this value of  $\tau^t$  in (18), we obtain (7).